Downhole and MASW Measurements of Shear- and Compression-Waves Velocities at Al Maabar- Aqaba region-South Jordan.

Aqaba-Jordan

PURPOSE

This report describes the procedures and results of a series of downhole measurements of shear- and compression-wave velocities and MASW survey performed as part of geotechnical Project at the site of Al Maabar port-shaeikh Zayed city-Aqaba.

1. Introduction.

Downhole seismic and MASW surveying is an important field methods for determining key *in-situ* subsurface information for earthquake engineering, soil and rock properties and other geotechnical site investigations. Downhole and MASW surveys are undertaken to measure the vertical distribution of seismic velocity in the earth.

Downhole survey provides detailed information on stratigraphy and the engineering properties of subsurface soils and rock that is not available from surface seismic surveys. Shear-wave velocity profiles obtained from downhole and MASW surveys are routinely incorporated in site response modeling for earthquake hazard evaluation and structural design.

Planning new constructions such as bridges, sky scrapers, dams, wind turbine and others demand detailed knowledge of subsurface structures over an area mostly larger than the footprint of the construction to be placed. Standard downhole and MASW tests for P and S waves can meet civil engineering demands after required elastic parameters such as shear velocity, compression velocity, poisson ratio, young modulus and shear modulus. Thus, parameters derived from geophysical testing are will play an important role in future helping to design constructions on save ground.

2. Downhole testing:

Like seismic refraction and MASW, the downhole seismic method is a method that uses the properties of acoustic waves to measure the velocity of the materials through which the waves travel. Unlike seismic refraction and MASW, downhole seismic requires a borehole in which to measure the seismic arrivals.

Downhole method is the traditional method used to obtain shear wave and p-wave velocities profiles of the subsurface for geotechnical design, and as such is commonly

used for calculations of Vs30, liquefaction assessment, and calculation of geotechnical design parameters.

Comparing Downhole shear wave with estimated shear wave refraction, MASW and ReMi, this method provides the highest resolution in the shear wave profile. Because refraction and ReMi use travel time to measure the seismic velocity of a material. MASW method measured Rayleigh and Love waves, by knowing these velocities the shear wave velocity can be estimated, the difference between downhole and MASW results raining between 15% to 35%. (Robert A. Bauer, Shear Wave Velocity, Geology and Geotechnical Data of Earth Materials in the Central U.S. Urban Hazard Mapping Areas, 2007, Technical Report).

In addition and unlike seismic refraction or MASW, this method measure the travel time of the direct wave, and as a result do not have difficulty resolving hidden layers. In fact, the downhole test can easily detect thin layers and velocity inversions in the subsurface.

The scope of boreholes condition is shown in chronological order in Table 1.

Table 1.Discribtion of Downhole seismic Boreholes.

Borehole	Casing	Filling	Depth range (m)	Survey mode	Source	Date
BH-DS1	**PVC**	**Grout**	**2-11**	**P & S**	**Sledge hammer & beam**	**25-06-13**
BH-DS2	**PVC**	**Grout**	**2-11**	**P & S**	**Sledge hammer & beam**	**25-06-13**
BH-DS3	**PVC**	**Grout**	**2-11**	**P & S**	**Sledge hammer & beam**	**25-06-13**
BH-DS4	**PVC**	**Grout**	**2-11**	**P & S**	**Sledge hammer & beam**	**25-06-13**
BH-DS5	**PVC**	**Grout**	**2-11**	**P & S**	**Sledge hammer & beam**	**25-06-13**

2-1. Downhole Seismic Technique.

In downhole seismic survey a triaxial geophone (photo.1) transducer is incrementally lowered down a borehole while seismic waves are generated from the surface. Based on the nature of the seismic waves when they reach the geophone, information on stratigraphy and seismic response can be deduced.

Photo.1. show triaxial geophone.

Downhole seismic velocity data are utilized in a variety of geotechnical site investigations, including earthquake site response modeling, foundation design for dynamic (vibratory) loads, estimating pile depth, and rock quality assessment. Downhole seismic data provides detailed information on stratigraphy and the engineering properties of subsurface soils and rock that is not available from surface seismic surveys.

A downhole seismic survey is conducted by measuring the time for seismic waves generated by an impulsive source at the surface to travel to a sensor located at a sequence of depths in the borehole. The sensor consists of three geophones arranged in an X-Y-Z pattern. Two orthogonal horizontal geophones are used to detect shear-wave (S-wave) arrivals and a vertical geophone is used to detect compression-wave

(P-wave) arrivals. At each measurement level, the sensor assembly is locked to the borehole wall using a clamping mechanism.

2-2. Procedures.

The standard procedure for a downhole velocity survey is to measure the travel times of signals from an impulsive source of energy at the surface to a sequence of measurement points in the borehole. The corresponding plot of travel time versus depth is then converted to velocity versus depth by computing slopes of the interpreted major straight-line segments of the plotted data.

The compression and shear waves source was a 10-Kg sledgehammer striking the ends of wood beam (15*15cm and 2.4m length), with steel ends and placed on 2 m distance from the borehole. The front wheels of a heavy vehicle were driven up onto the beam to hold it in firm contact with the ground (photo.2). The sledgehammer has an impact sensor attached to its handle near the head that generates a zero-time signal for the seismograph.

Photo.2. Shows compression and shear-waves source.

All signals were recorded with a Dolang Seismograph Model DBS280B digital seismograph (Dolang, Inc., Genova, Italy) configured to record as many as 24 channels of data.The system components are listed in Table2, Photo3 and the data acquisition parameters are listed in Table 3.

Table 2. Components of the seismic recording system.

1	Dolang Seismograph Model DBS280B digital seismograph 24 channels.
2	Downhole geophone 14-Hz, with three components (*X*,*Y*,*Z*: longitudinal, transversal, vertical)
3	10-kg hand-held hammer and wooden beam 240-cm in length and 15*15 cm, flattened at surface in contact with the ground surface.

Photo.3. Shows Dolang seismic system.

Table 3. Recording parameters for downhole seismic survey.

Borehole geophone type	14 Hz, *(X,Y,Z)* three-component
Number of records at each depth level	2
Number of channels per record	3
First channel	*Z* component
Second channel	*X* component
Third channel	*Y* component
Depth interval for recording	1 m
Number of samples	1024
Sampling rate	128 microsecond
Recording time	0.131 sec
Recording format	SU & SGY

2-3. Data Processing.

The raw, unfiltered signals acquired in a velocity survey are transferred directly to the notebook, filtering is applied only during playback. In general, filters are employed to suppress noise or interference that may be superimposed on a shear or compression wave signal. The sources of interference are not always apparent but may include mechanical noise from nearby traffic, generators, or structures, multiple travel paths of the downward traveling pulse, reverberations and reflections due to changes in acoustic impedance at the stratigraphic boundaries, and questionable coupling of the casing to the surrounding material.

The frequency range of a typical shear wave is approximately 30 Hz to 70 Hz. As the pass band of a filter becomes more restrictive, it also diminishes the amplitude of the signal along with that of the interference. It is often a matter of judgment how much

filtering to apply to the raw signals and this judgment is guided by inspection of the raw recorded signals. As a general rule, the less filtering, the better.

Filtering was accomplished by using the digital filters built into the operating system of the DBS280B seismograph. Different low-pass was applied for shear-wave signals in the survey and a 400-Hz low-pass was used for all compression wave surveys using the DBS280B software during playback.

First arrivals the slant times for P and S waves are picked on the field records. The times are then converted to vertical times using the depth **H** and the distance **X** of the source from the center of the borehole figure.1.

$$\mathbf{T} \text{ vertical} = \mathbf{cos\theta} \times \mathbf{T} \text{ measured}$$

Where $\boldsymbol{\theta} = \mathbf{tg^{-1}(X/H),}$

X is the distance from the source to borehole,

H is the depth of the sensor.

The interval velocity is computed by dividing the difference in depth between the geophones **Δh = (h2-h1), by** the difference in arrival times **Δt = (t2-t1).**

The compression and the shear velocities are calculated as follows:

$\mathbf{V = \Delta h/\Delta t}$ Where **V** is the velocity of P or S wave,

Δh is the thickness of the geological layer in m,

Δt is the difference in time of the top and base of the layer in ms.

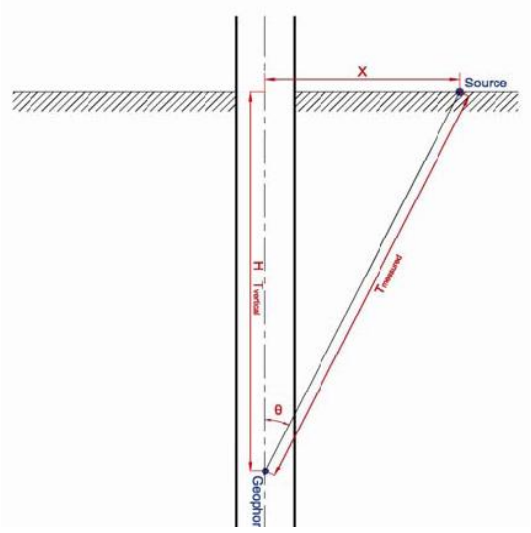

Figure.1.

The first arrival times for P wave and S wave picked using the DBS280B software package after merge and sort data which recorded using right head of wooden beam as a source of the signals, another picking for P wave and S wave utilizing the merged

and sorted data which recorded using left head of wooden beam as a source of the signals. The first record started at highest depth to reach 2 m. The corrected vertical time made automatically.

Dynamic properties (Shear velocity Vs, Compressional velocity Vp, Shear Modulus, Poisson Ratio and Young Modulus) of geotechnical material calculated based on Vs and Vp values using equations below.

$$\textbf{Poisson's Ratio } \nu = (VP^2 - 2VS^2)/2(VP^2 - VS^2)$$

$$\textbf{Shear Modulus } G = \rho V_s^2$$

$$\textbf{Young's Modulus } E = 2G(1+\nu)$$

Where ρ = force density

2-4. Boreholes Measurements.

Two records, each with three channels were acquired at 1 m depth interval within a depth range of 2-11 m inside boreholes with PVC casing and backfilled in order for the wave motion to be transferred from the soil column to the geophone. The SU format, which is one of standard in engineering seismology, was used to record the data. The field work using the integrated system described in Table 3 was carried out as follows:

(1) The seismic source placed 2-m away from the well head.

(2) The geophone probe was lowered to the maximum depth of recording (11 m) using the cable connected to the geophone control unit and tension was applied to the clamp so as to achieve a firm contact with the borehole perimeter.

(3) The signal was transmitted via the geophone cable to the Dolang geophone control unit. The (*Z,X,Y:* vertical, longitudinal, transversal) components defined by the control unit and each recorded on one channel (*Z*: first channel, *X:* second channel, and *Y:* third channel) were then transmitted to the Dolang recording unit, and were converted from analog to digital form. Subsequently, this three-channel digital signal was transmitted to the laptop from the recording unit.

(4)The following records were acquired in the order listed below:

First record: An P wave and S wave generated by a *horizontal impact* using the hand-held hammer applied to one end of a plank, placed 2-m away from the well head, and the (*Z,X,Y*) components were each recorded on three channels. Only the first channel of this record that records the *Z* component, the second channel and third channel of

this record that records the S wave (channel 2 for X component and channel 3 for Y component). Second record: Another shot applied to opposite end of the plank in the opposite direction as for the second record, and the (Z,X,Y) components were each recorded on three channels.

(5) The tension applied to the clamp on the geophone probe was slightly released and the probe was pulled by 1 m up to the next depth level, then tension again was applied to the clamp so as to achieve a firm contact with the borehole perimeter. The recording was continued in the manner described above.

Records files merges and sorted in one file with 10 channels for +P, +S1 and +S2 (1^{st} record at each interval depth), again, records files merges and sorted in one file with 10 channels for -P, -S1 and -S2 (2^{ed} record at each interval depth). These steps applied on all boreholes.

2-5. Results.

2-5-1. BH-DS1.

Merge and sorted data in BH-DS1 for the first shot and second shot for each depth interval illustrated in figure.2 and figure.3.

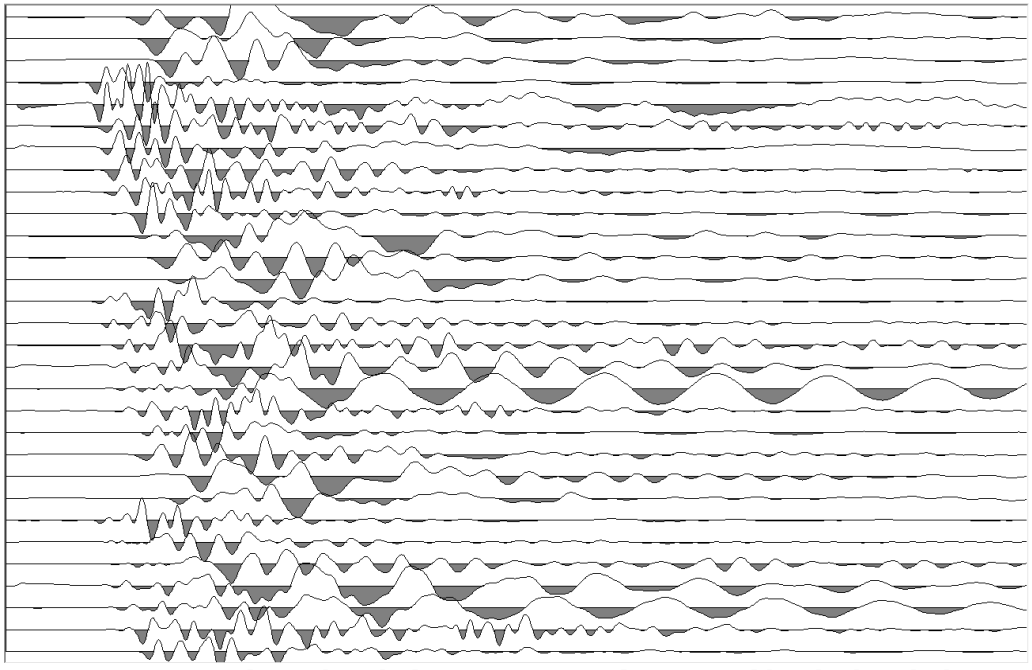

Figure.2. +P, +S1 and +S2 borehole seismic records acquired by the borehole survey at BH-DS1.

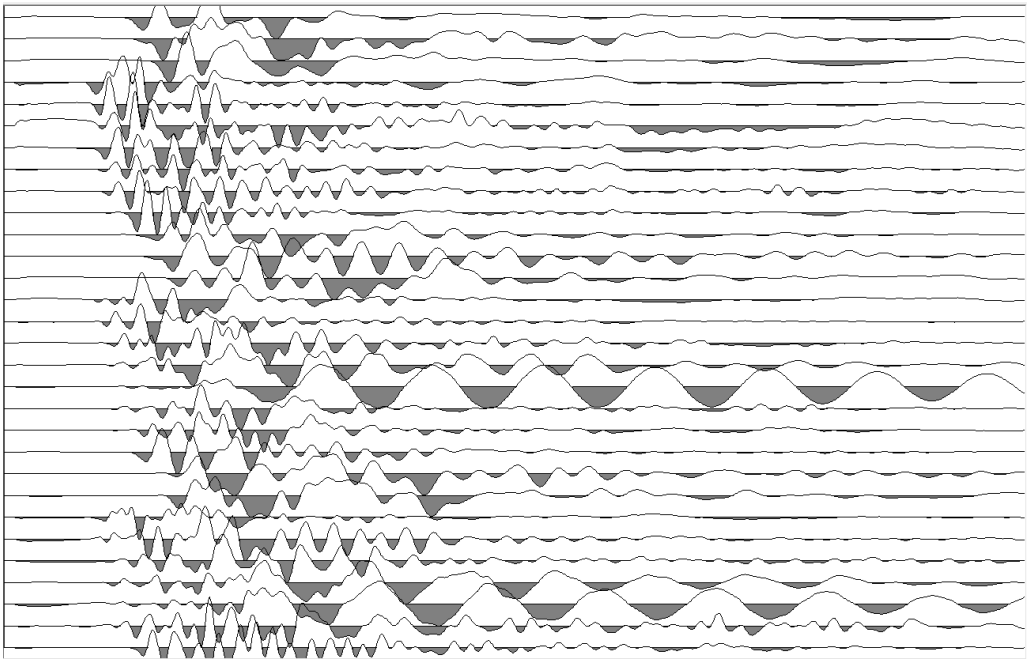

Figure.3. -P, -S1 and -S2 borehole seismic records acquired by the borehole survey at BH-DS1.

Table.4. shows P and S waves first measured arrival time, corrected time for P and S waves and corrected distance between source and receiver.

Table.4. measured travel time, corrected time and corrected distance between source and receiver.

Depth (m)	SR (m)	Tp (mSec)	Tpcor (mSec)	Ts (mSec)	Tscor (mSec)
2	2.8284	13.1	9.263188	22	15.5565
3	3.6056	15.1	12.56379	25.5	21.217
4	4.4721	17.4	15.56316	30.5	27.28025
5	5.3852	10	9.284706	18.2	16.89817
6	6.3246	10.9	10.34057	20.6	19.54274
7	7.2801	11.7	11.24985	23.4	22.49969
8	8.2462	11.8	11.4477	25	24.2536
9	9.2195	12.2	11.90954	27.8	27.13813
10	10.198	12.4	12.15925	30.1	29.51559
11	11.1803	15.7	15.44681	31.7	31.18879

SR corrected distance between source and receiver.
Tp measured compression wave travel time.
Ts measured shear wave travel time
Tpcor corrected compression wave travel time.
Tscor corrected shear wave travel time.

Corrected travel time graph shown in figure.4.

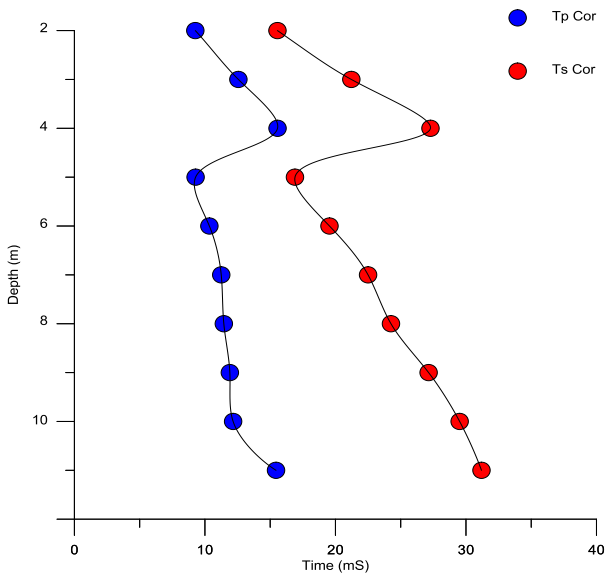

Figure.4. Illustrate corrected travel time graph for P wave and S wave (BH-DS1).

Dynamic properties for BH-DS1 are shown in table.5. and variation between dynamic properties shown in table.6.

Table.5. Dynamic properties of layers with depth using downhole test at BH-DS1.

Depth (m)	V_p (m/sec)	V_s (m/sec)	ρ (T/mc)	ν	G (MPa)	E (MPa)
2	215.908397	128.563636	1.918	0.225327	31.70187	77.69034
3	238.781457	141.396078	1.817	0.23	36.32701	89.36441
4	257.017241	146.62623	1.716	0.258753	36.89272	92.87764
5	538.52	295.89011	1.97	0.283774	172.4754	442.839
6	580.238532	307.019417	2.072	0.30558	195.3086	509.9821
7	622.230769	311.115385	2.0118	0.333333	194.7277	519.2739
8	698.830508	329.848	2.181	0.356678	237.2922	643.8582
9	755.696721	331.636691	2.006	0.380737	220.6257	609.2522
10	822.419355	338.803987	2.066	0.3978	237.1523	662.9829
11	712.121019	352.690852	2.174	0.337493	270.4257	723.3851

Table.6. Illustrate variation of dynamic properties with depth at BH-DS1.

Depth(m)	ΔVp (m/sec)	ΔVs (m/sec)	Δν	ΔG (MPa)	ΔE (MPa)
2	-	-	-	-	-
3	22.87306	12.8324421	0.004672	4.625139	11.67407
4	18.2357844	5.23015108	0.028754	0.565705	3.51323
5	281.502759	149.26388	0.025021	135.5827	349.9613
6	41.7185321	11.1293076	0.021806	22.83325	67.14315
7	41.9922371	4.09596714	0.027753	-0.58091	9.291793
8	76.5997392	18.7326154	0.023345	42.56443	124.5843
9	56.8662128	1.78869065	0.024059	-16.6665	-34.606
10	66.7226335	7.16729606	0.017063	16.52661	53.73076
11	-110.298336	13.886865	-0.06031	33.27338	60.40219

*ΔVp, ΔVs, ΔG, DE & Dν variation of dynamic properties with depth.

2-5-2. BH-DS2.

Merge and sorted data in BH-DS2 for the first shot and second shot for each interval depth illustrated in figure.5. and figure.6.

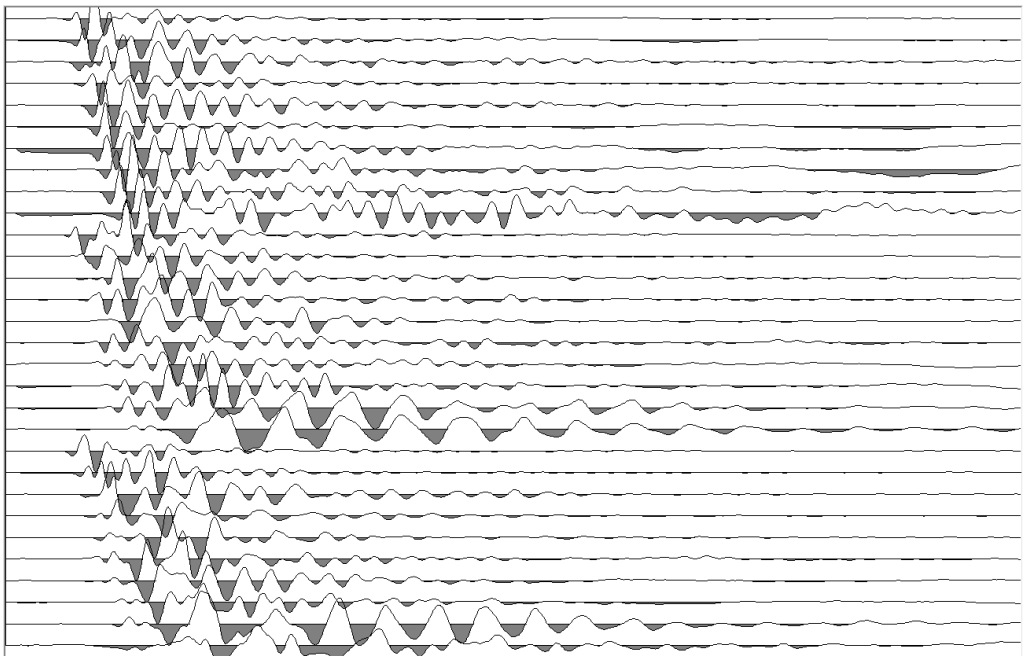

Figure.5. +P, +S1 and +S2 borehole seismic records acquired by the borehole survey at BH-DS2.

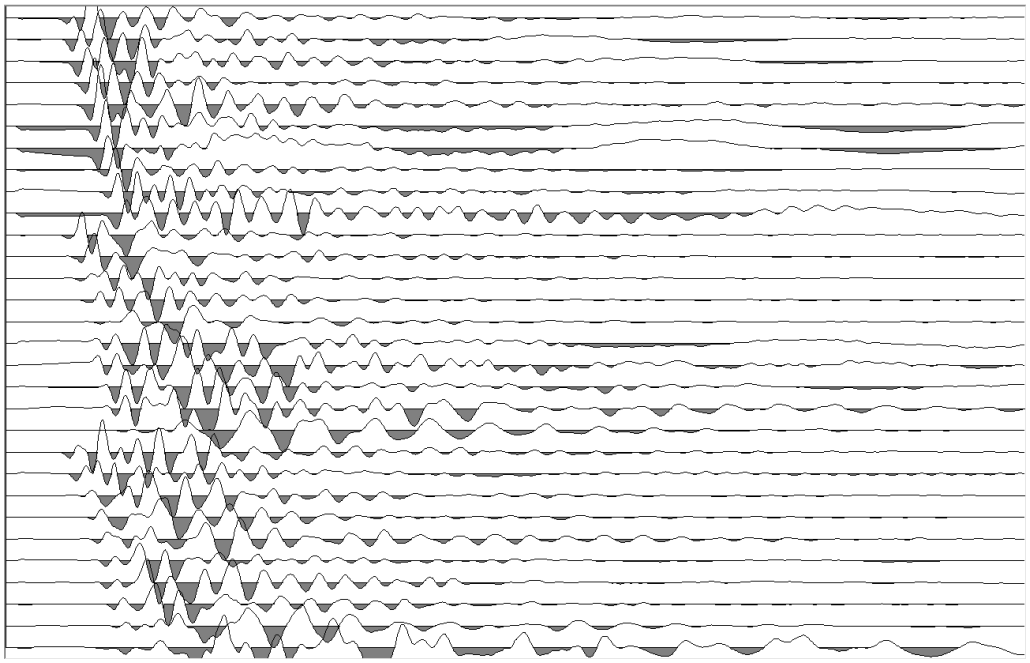

Figure.6. -P, -S1 and -S2 borehole seismic records acquired by the borehole survey at BH-DS2.

Table.7. shows P and S first measured arrival time, corrected time for P and S and corrected distance between source and receiver.

Table.7. measured travel time, corrected time and corrected distance between source and receiver.

Depth (m)	SR (m)	Tp (msec)	Tpcor (msec)	Ts (msec)	Tscor (msec)
2	2.8284	12.8	9.051054	20	14.14227
3	3.6056	14	11.64855	21.6	17.97204
4	4.4721	15.2	13.5954	25.5	22.80808
5	5.3852	16.8	15.59831	27.9	25.90433
6	6.3246	17.6	16.69671	29.4	27.89109
7	7.2801	19.9	19.13435	37.3	35.86489
8	8.2462	20.7	20.08198	38.9	37.73859
9	9.2195	22.3	21.76908	41.3	40.31672
10	10.198	23.1	22.6515	46.8	45.89135
11	11.1803	24.7	24.30167	50.7	49.88238

SR corrected distance between source and receiver.
Tp measured compression wave travel time.
Ts measured shear wave travel time
Tpcor corrected compression wave travel time.
Tscor corrected shear wave travel time.

Corrected travel time graph shown in figure.7.

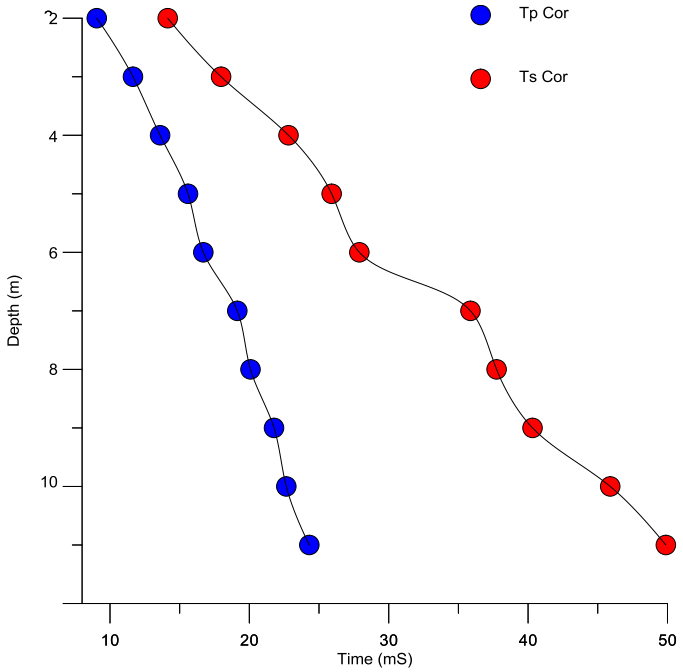

Figure.7. Illustrate travel time graph for P wave and S wave (BH-DS2).

Dynamic properties for BH-DS2 are shown in table.8. and variation between dynamic properties shown in table.9.

Table.8. Dynamic properties of layers with depth using downhole test at BH-DS2.

Depth (m)	V_p (m/sec)	V_s (m/sec)	ρ (T/mc)	ν	G (MPa)	E (MPa)
2	220.96875	141.42	1.898	0.153117	37.95927	87.54293
3	257.542857	166.925926	2.013	0.137788	56.09076	127.6388
4	294.217105	175.376471	1.889	0.224434	58.0998	142.2787
5	320.547619	193.017921	2.033	0.215581	75.74128	184.1394
6	359.352273	215.122449	2.165	0.220736	100.1912	244.6138
7	365.834171	195.176944	1.631	0.301056	62.13138	161.6728
8	398.36715	211.984576	2.161	0.302488	97.10985	252.9689
9	413.430493	223.232446	2.046	0.294236	101.9578	263.9148
10	441.471861	217.905983	1.74	0.338947	82.62045	221.2488
11	452.643725	220.518738	1.864	0.344397	90.64355	243.7218

Table.9. Illustrate variation of dynamic properties with depth at BH-DS2.

Depth(m)	ΔVp (m/sec)	ΔVs (m/sec)	Δv	ΔG (MPa)	ΔE (MPa)
2	-	-	-	-	-
3	36.5741071	25.5059259	-0.01533	18.13149	40.0959
4	36.6742481	8.45054466	0.086646	2.009031	14.63991
5	26.3305138	17.6414506	-0.00885	17.64148	41.86064
6	38.8046537	22.1045278	0.005154	24.44987	60.47445
7	6.48189813	-19.9455053	0.08032	-38.0598	-82.941
8	32.5329789	16.8076321	0.001432	34.97847	91.29607
9	15.0633435	11.2478697	-0.00825	4.847903	10.94596
10	28.0413682	-5.32646261	0.044711	-19.3373	-42.666
11	11.1718632	2.61275477	0.005449	8.023099	22.47292

*ΔVp, ΔVs, ΔG, ΔE & $\Delta\nu$ variation of dynamic properties with depth.

2-5-3. BH-DS3.

Merge and sorted data in BH-DS3 for the first shot and second shot for each interval depth illustrated in figure.8. and figure.9.

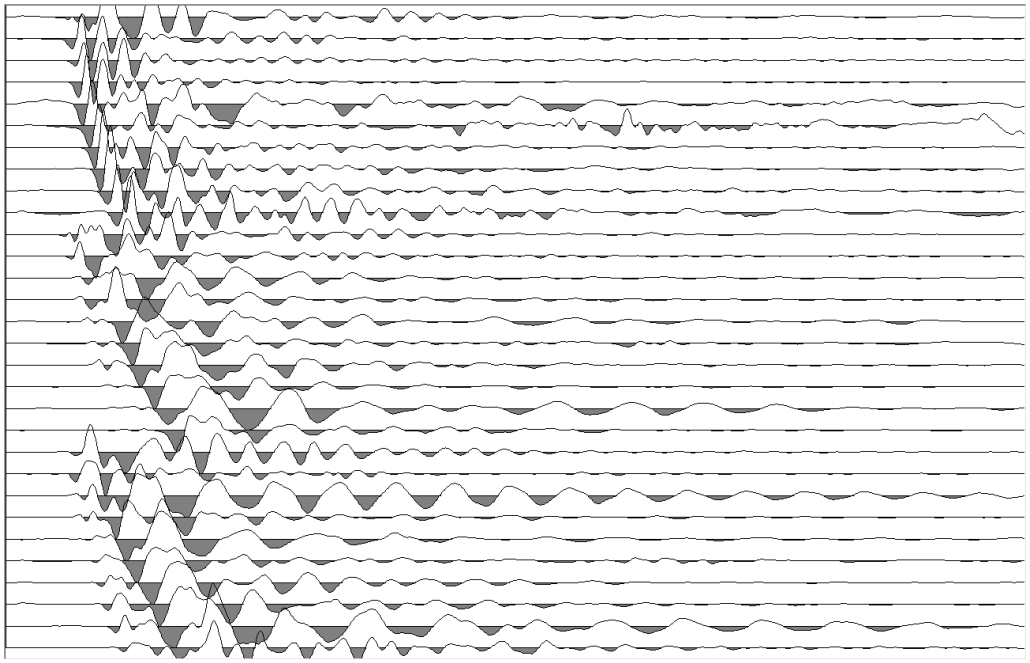

Figure.8. +P, +S1 and +S2 borehole seismic records acquired by the borehole survey at BH-DS3.

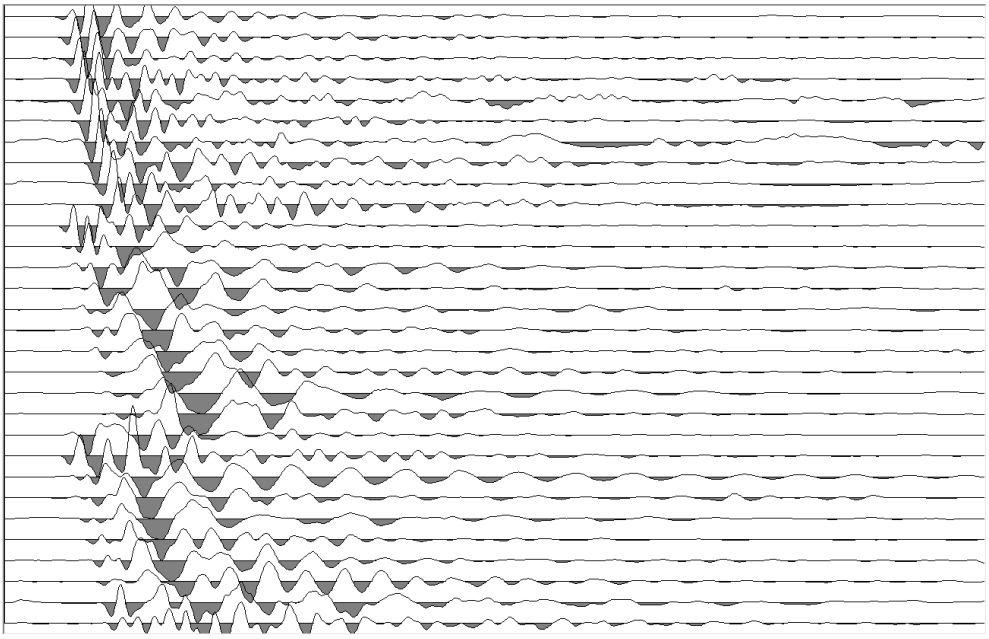

Figure.9. -P, -S1 and -S2 borehole seismic records acquired by the borehole survey at BH-DS3.

Table.10. shows P and S first measured arrival time, corrected time for P and S and corrected distance between source and receiver.

Table.10. measured travel time, corrected time and corrected distance between source and receiver.

Depth (m)	SR (m)	Tp (msec)	Tpcor (msec)	Ts (msec)	Tscor (msec)
2	2.8284	12.8	9.051054	22.1	15.62721
3	3.6056	13.2	10.98292	23.9	19.88573
4	4.4721	14.1	12.61152	26.2	23.43418
5	5.3852	15.1	14.01991	28.3	26.27572
6	6.3246	16.2	15.36856	30	28.4603
7	7.2801	17	16.34593	31.4	30.19189
8	8.2462	19.8	19.20885	34.8	33.76101
9	9.2195	21.5	20.98812	36.8	35.92386
10	10.198	23.9	23.43597	39.9	39.12532
11	11.1803	23.6	23.21941	42.1	41.42107

SR corrected distance between source and receiver.
Tp measured compression wave travel time.
Ts measured shear wave travel time
Tpcor corrected compression wave travel time.
Tscor corrected shear wave travel time.

Corrected travel time graph shown in figure.10.

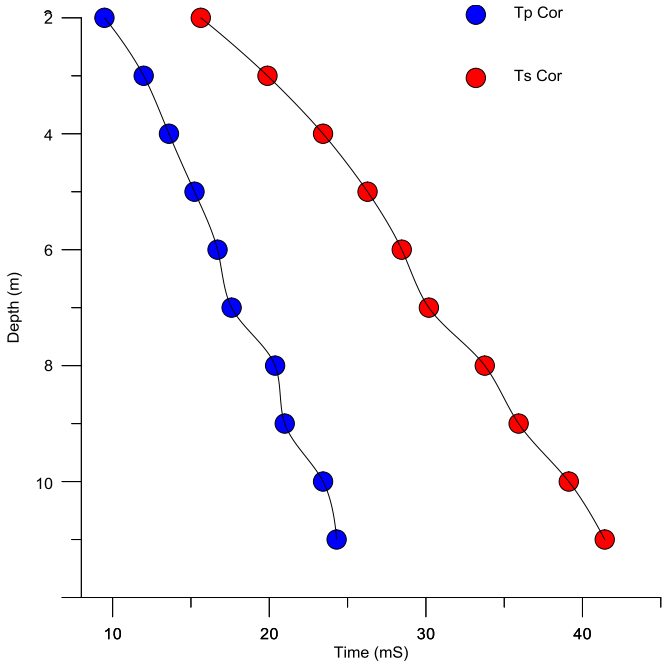

Figure.10. Illustrate travel time graph for P wave and S wave (BH-DS3).

Dynamic properties for BH-DS3 are shown in table.11. and variation between dynamic properties shown in table.12.

Table.11. Dynamic properties of layers with depth using downhole test at BH-DS3.

Depth (m)	V_p (m/sec)	V_s (m/sec)	ρ (T/mc)	ν	G (MPa)	E (MPa)
2	220.96875	127.9819	1.898	0.247605	31.08804	77.57115
3	273.151515	150.861925	1.961	0.280538	44.63103	114.3034
4	317.170213	170.69084	1.939	0.296147	56.49347	146.4476
5	356.635762	190.289753	2.127	0.300997	77.01907	200.4031
6	390.407407	210.82	2.28	0.294184	101.3348	262.2917
7	428.241176	231.850318	2.068	0.292671	111.1645	287.3981
8	416.474747	236.95977	1.958	0.260659	109.9416	277.1977
9	428.813953	250.529891	2.171	0.240888	136.2633	338.1751
10	426.694561	255.588972	1.959	0.220215	127.9731	312.3093
11	473.741525	265.565321	1.857	0.270883	130.9648	332.882

Table.12. Illustrate variation of dynamic properties with depth at BH-DS3.

Depth(m)	ΔVp (m/sec)	ΔVs (m/sec)	Δν	ΔG (MPa)	ΔE (MPa)
2	-	-	-	-	-
3	52.1827652	22.8800242	0.032933	13.54299	36.73226
4	44.0186976	19.828915	0.015609	11.86244	32.14423
5	39.4655488	19.598913	0.00485	20.52561	53.95548
6	33.7716458	20.5302473	-0.00681	24.31569	61.88855
7	37.8337691	21.0303185	-0.00151	9.829686	25.10645
8	-11.766429	5.10945164	-0.03201	-1.22288	-10.2004
9	12.339206	13.5701212	-0.01977	26.32174	60.97737
10	-2.11939282	5.05908113	-0.02067	-8.29022	-25.8658
11	47.0469648	9.97634823	0.050669	2.991722	20.57271

*ΔVp, ΔVs, ΔG, ΔE & $\Delta\nu$ variation of dynamic properties with depth.

2-5-4. BH-DS4.

Merges and sorted data in BH-DS4 for the first shot and second shot for each interval depth illustrated in figure.11. and figure.12.

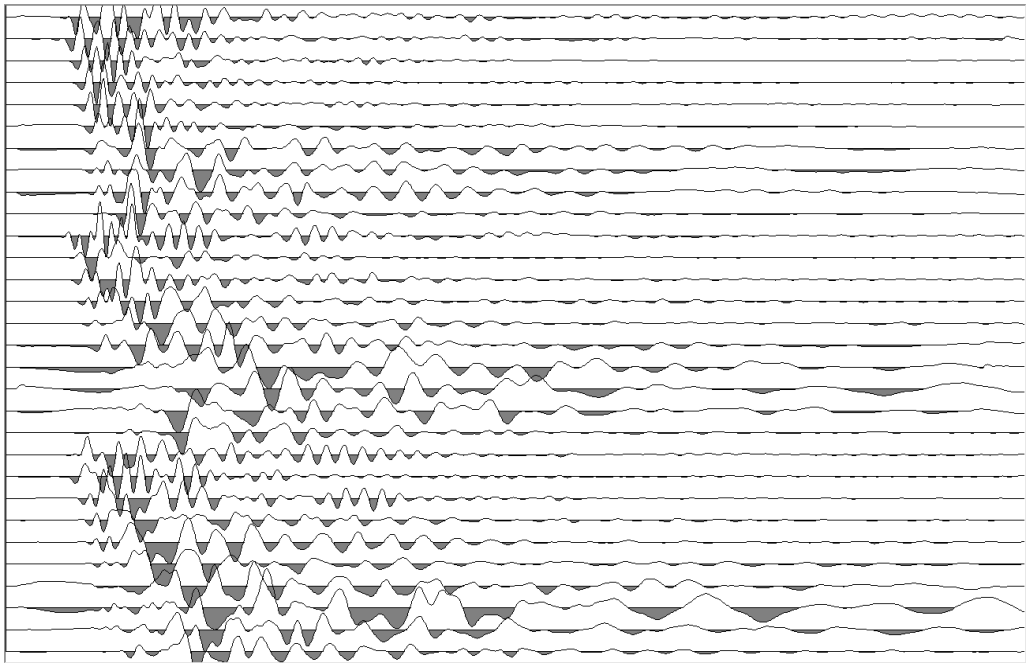

Figure.11. +P, +S1 and +S2 borehole seismic records acquired by the borehole survey at BH-DS4.

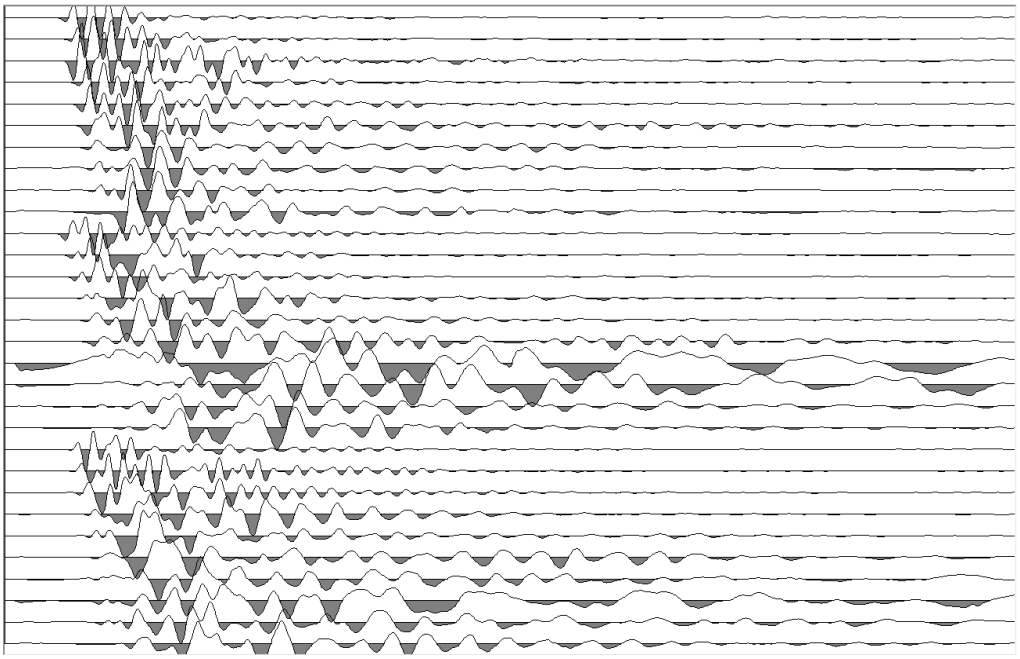

Figure.12. -P, -S1 and -S2 borehole seismic records acquired by the borehole survey at BH-DS4.

Table.13. shows P and S first measured arrival time, corrected time for P and S and corrected distance between source and receiver.

Table.13. measured travel time, corrected time and corrected distance between source and receiver.

Depth (m)	SR (m)	Tp (msec)	Tpcor (msec)	Ts (msec)	Tscor (msec)
2	2.8284	11.5	8.131806	19.5	13.78871
3	3.6056	13.2	10.98292	22.7	18.88729
4	4.4721	15	13.41652	25.9	23.16585
5	5.3852	16.5	15.31977	28.2	26.18287
6	6.3246	18	17.07618	29.5	27.98596
7	7.2801	19.1	18.36513	33.4	32.11494
8	8.2462	19.9	19.30586	39.7	38.51471
9	9.2195	21.5	20.98812	41.3	40.31672
10	10.198	22.3	21.86703	43.6	42.75348
11	11.1803	26.2	25.77748	49.2	48.40657

SR corrected distance between source and receiver.
Tp measured compression wave travel time.
Ts measured shear wave travel time
Tpcor corrected compression wave travel time.
Tscor corrected shear wave travel time.

Corrected travel time graph shown in figure.13.

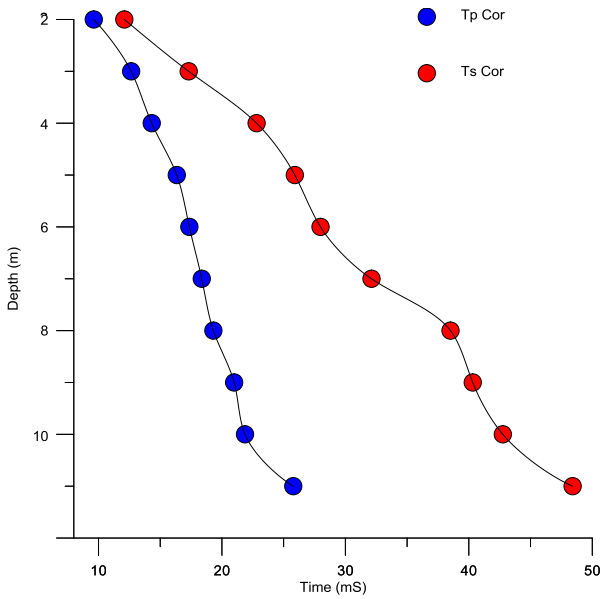

Figure.13. Illustrate travel time graph for P wave and S wave (BH-DS4).

Dynamic properties for BH-DS4 are shown in table.14. and variation between dynamic properties shown in table.15.

Table.14. Dynamic properties of layers with depth using downhole test at BH-DS4.

Depth (m)	V_p (m/sec)	V_s (m/sec)	ρ (T/mc)	ν	G (MPa)	E (MPa)
2	245.947826	145.046154	1.961	0.233367	41.25628	101.7683
3	273.151515	158.837004	1.891	0.244554	47.70841	118.7513
4	298.14	172.667954	1.838	0.24765	54.79854	136.7388
5	326.375758	190.964539	2.033	0.239718	74.13834	183.8212
6	351.366667	214.39322	2.151	0.203432	98.86954	237.9656
7	381.157068	217.967066	1.892	0.257036	89.88824	225.9856
8	414.38191	207.712846	1.705	0.332211	73.56159	195.999
9	428.813953	223.232446	2.165	0.314125	107.8878	283.5561
10	457.309417	233.899083	2.058	0.322861	112.5907	297.8836
11	426.729008	227.24187	1.726	0.302087	89.12869	232.1067

Table.15. Illustrate variation of dynamic properties with depth at BH-DS4.

Depth(m)	ΔVp (m/sec)	ΔVs (m/sec)	Δν	ΔG (MPa)	ΔE (MPa)
2	-	-	-	-	-
3	27.2036891	13.7908506	0.011187	6.452129	16.98308
4	24.9884848	13.8309493	0.003097	7.090135	17.9875
5	28.2357576	18.2965853	-0.00793	19.3398	47.08239
6	24.9909091	23.4286813	-0.03629	24.7312	54.1444
7	29.7904014	3.57384553	0.053604	-8.9813	-11.9801
8	33.2248415	-10.2542195	0.075174	-16.3267	-29.9865
9	14.4320439	15.5195992	-0.01809	34.32626	87.55709
10	28.4954636	10.666637	0.008736	4.702822	14.32743
11	-30.5804094	-6.65721265	-0.02077	-23.462	-65.7769

*ΔVp, ΔVs, ΔG, ΔE & $\Delta\nu$ variation of dynamic properties with depth.

2-5-5. BH-DS5.

Merges and sorted data in BH-DS5 for the first shot and second shot for each interval depth illustrated in figure.14. and figure.15.

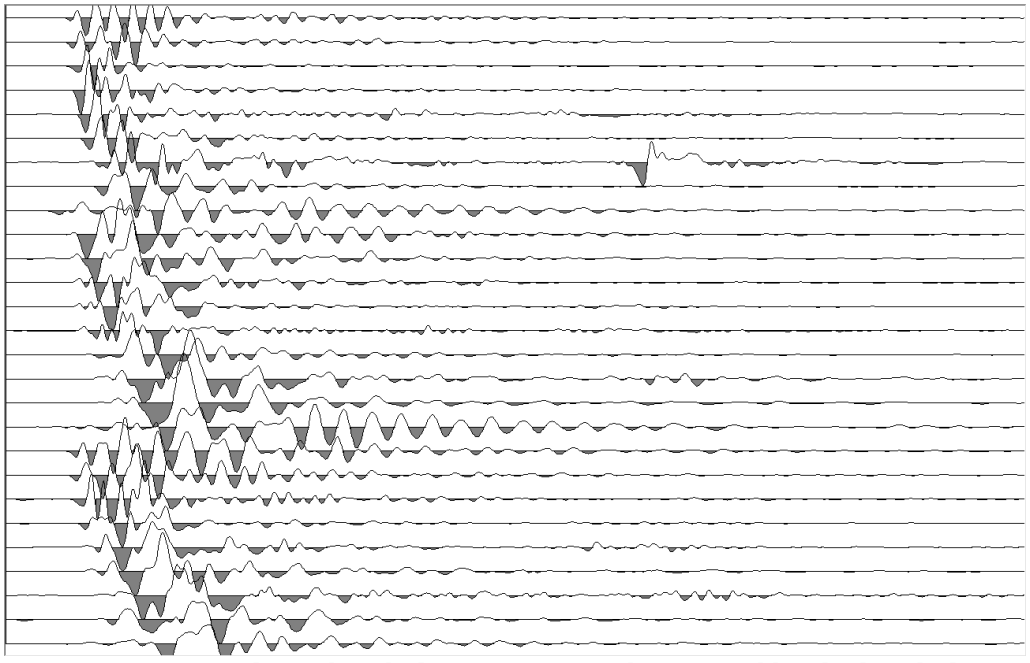

Figure.14. +P, +S1 and +S2 borehole seismic records acquired by the borehole survey at BH-DS5.

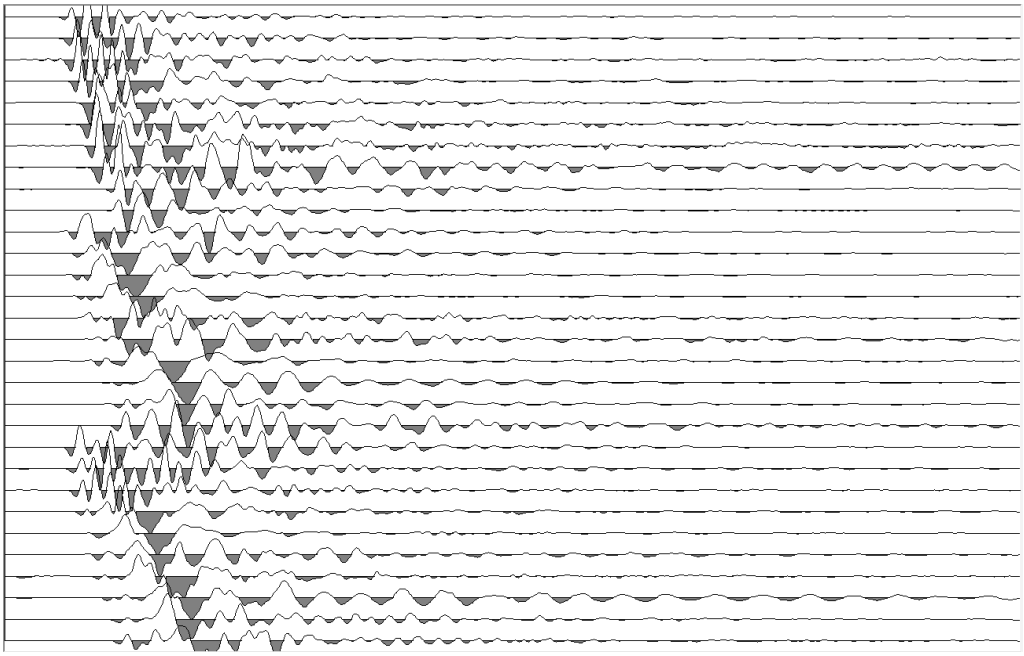

Figure.15. -P, -S1 and -S2 borehole seismic records acquired by the borehole survey at BH-DS5.

Table.16. shows P and S first measured arrival time, corrected time for P and S and corrected distance between source and receiver.

Table.16. measured travel time, corrected time and corrected distance between source and receiver.

Depth (m)	SR (m)	Tp (msec)	Tpcor (msec)	Ts (msec)	Tscor (msec)
2	2.8284	11.1	7.848961	18.4	13.01089
3	3.6056	12.2	10.15088	21	17.47282
4	4.4721	13	11.62765	22	19.67756
5	5.3852	14.6	13.55567	24.6	22.84038
6	6.3246	16	15.17883	27.5	26.08861
7	7.2801	17.2	16.53823	29.9	28.74961
8	8.2462	18.5	17.94766	32.1	31.14162
9	9.2195	20.1	19.62145	34.9	34.06909
10	10.198	23.5	23.04373	39.5	38.73308
11	11.1803	25.2	24.79361	42.5	41.81462

SR corrected distance between source and receiver.
Tp measured compression wave travel time.
Ts measured shear wave travel time
Tpcor corrected compression wave travel time.
Tscor corrected shear wave travel time.

Corrected travel time graph shown in figure.16.

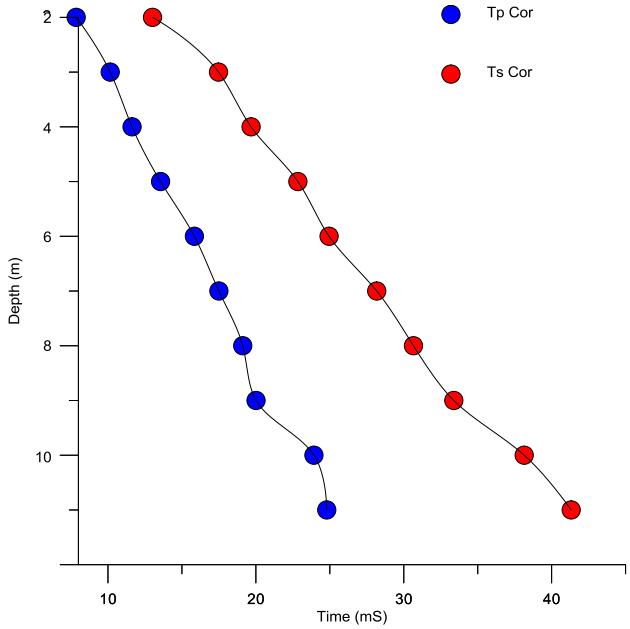

Figure.16. Illustrate travel time graph for P wave and S wave (BH-DS5).

Dynamic properties for BH-DS5 are shown in table.17. and variation between dynamic properties shown in table.18.

Table.17. Dynamic properties of layers with depth using downhole test at BH-DS5.

Depth (m)	V_p (m/sec)	V_s (m/sec)	ρ (T/mc)	ν	G (MPa)	E (MPa)
2	254.810811	153.717391	1.931	0.213931	45.62767	110.7777
3	295.540984	171.695238	1.956	0.245277	57.66142	143.6088
4	344.007692	203.277273	2.098	0.231746	86.69282	213.5671
5	368.849315	218.910569	2.091	0.228112	100.2046	246.1249
6	395.2875	229.985455	2.146	0.244128	113.509	282.4395
7	423.261628	243.481605	1.987	0.252712	117.7959	295.1288
8	445.740541	256.890966	2.069	0.25133	136.5395	341.7117
9	458.681592	264.169054	2.026	0.251837	141.385	353.9818
10	433.957447	258.177215	1.803	0.226066	120.1798	294.6969
11	443.662698	263.065882	1.887	0.228896	130.5873	320.9564

Table.18. Illustrate variation of dynamic properties with depth at BH-DS5.

Depth(m)	ΔVp (m/sec)	ΔVs (m/sec)	Δv	ΔG (MPa)	ΔE (MPa)
2	-	-	-	-	-
3	40.7301728	17.9778468	0.031346	12.03375	32.83117
4	48.4667087	31.5820346	-0.01353	29.0314	69.95824
5	24.8416228	15.6332964	-0.00363	13.51174	32.55782
6	26.4381849	11.0748854	0.016016	13.30448	36.31464
7	27.9741279	13.4961508	0.008585	4.28686	12.68924
8	22.4789126	13.4093604	-0.00138	18.74355	46.58294
9	12.9410515	7.27808871	0.000507	4.845545	12.27011
10	-24.7241452	-5.99183925	-0.02577	-21.2052	-59.2849
11	9.7052516	4.88866716	0.002829	10.40748	26.25947

*Δ**V**p, Δ**V**s, Δ**G**, Δ**E** & Δ**v** variation of dynamic properties with depth.

3. Multi-channel Analysis of Surface Waves (MASW).

As mentioned above, the Seismic shear-wave velocity is a key parameter for determining the elastic properties of soil and rock for geotechnical investigations. *In-situ* measurements of shear-wave velocity are traditionally made with seismic downhole method or through non-invasive methods such as Spectral Analysis of Surface Waves (SASW). A relatively new improvement to SASW known as Multi-channel Analysis of Surface Waves (MASW) allows shear-wave measurements to be made at multiple locations (e.g. along a profile line or survey grid) in a more efficient.

The benefits of MASW are immense. Shear-wave velocities can be measured to depths of 30 meter. The measurements are non-invasive and can provide coverage over large areas for reconnaissance investigations. It can identify features that other geophysical methods may miss, such as soft (low-velocity) layers below hard (high-velocity) layers.

As with all new geophysical methods, many are overselling it as a wonder-method that will solve all problems. However, as with all techniques, MASW has its advantages and limitations that should be recognized:

• MASW data should be processed and interpreted by geophysicists experienced with seismic methods.
• MASW works extremely well in areas with gradational velocity contrasts, such as variations in unconsolidated material and weathered rock. However, in areas where there is shallow hard rock or in areas with sharp layer boundaries, the method typically has moderate capability. Other methods such as seismic refraction would be more applicable to these situations.
• MASW can present as 1D and 2D cross-sections. It is important to keep in mind that the cross sections are made up of a series of interpolated 1D (not 2D) models. The horizontal resolution of the models depends on how the data were acquired (e.g. geophone and shot spacing).
• MASW is traditionally applied with active impulsive sources.
• As with any geophysical method, complimentary datasets from other geophysical methods or borings should be used to constrain the models and the interpretation.
A detailed description of the theory of the multichannel analysis of surface waves (MASW) method and typical field application can be found in Park et al. (1999), Xia et al. (1999), and Miller et al. (1999).

Richart el al. (1970) illustrated the relationship between the velocities of S-waves and Rayleigh waves propagating in an elastic half space. Sheriff (1991) suggested that ordinary values of Poisson's ratio range from 0 for very stiff solids to 0.5 for fluids. For that range of Poisson's ratio, a graph of the ratio of Rayleigh wave velocity to S-wave velocity versus the Poisson's ratio is plotted, and shown in figure 17.

The figure shows that Rayleigh wave velocity ranges from 0.87 to 0.96 of S-wave velocity. The properties of surface waves can be useful for estimating S-wave velocities of the near surface. The MASW method was applied to obtain a near surface S-wave velocity at a study area. The implementation of the MASW method involves recording Rayleigh waves on vertical component geophones, estimating phase-velocity dispersion curves for Rayleigh waves, and then inverting these dispersion curves to estimate S-wave velocity as a function of depth. The data was processed using SWAN software.

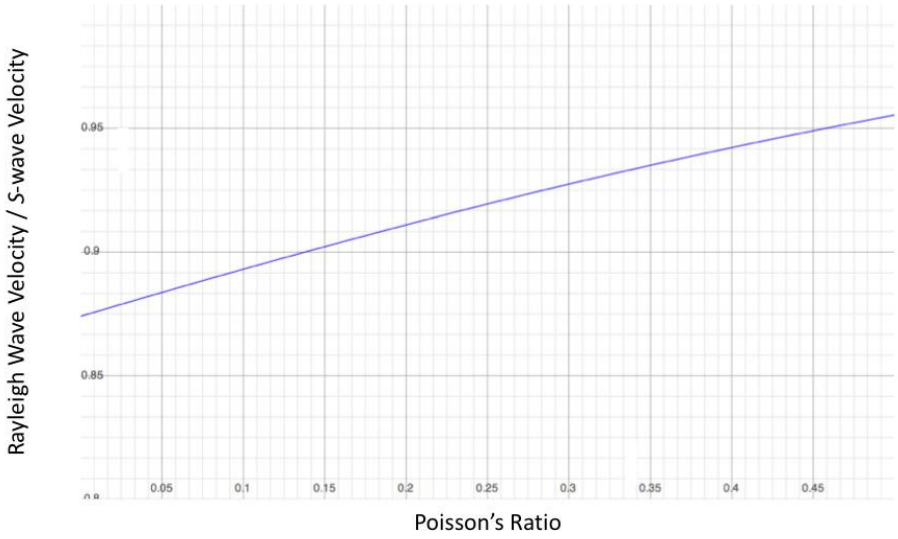

Figure 17. Ratio of Rayleigh wave velocity to S-wave velocity versus Poisson's ratios. Earth materials with Poisson's ratio of 0.5 to 0.0 have velocities that range from 0.84 to 0.96 of S-wave velocities.

3-1. General Acquisition Parameters

A 24-channel Dolang system (DBS280B) was used as the main recording device. One 4.5-Hz geophone was used as receiver at each station whose interval was 3 m. A total recording time of 2000 mS (2 Sec) was used with a 1 mS sampling interval. No acquisition filters were used.

3-2. General Procedure with MASW Method

A multiple number of receivers (usually 24) are deployed with even spacing along a linear survey line with receivers connected to a multichannel recording device (seismograph) (photo 4). Each channel is dedicated to recording vibrations from one receiver. One multichannel record (commonly called a shot gather) consists of a multiple number of time series (called traces) from all the receivers in an ordered manner.

Photo.4. Shows MASW profile.

3-3. (1-D and 2-D) Shear wave velocity (Vs).

One line selected for 1-D and 2-D Vs profiling, this line located within study area near the downhole bores. Five 24-channel shots gathers were acquired in the fixed source receiver mode. Mean of five field shots illustrated in figure 18.

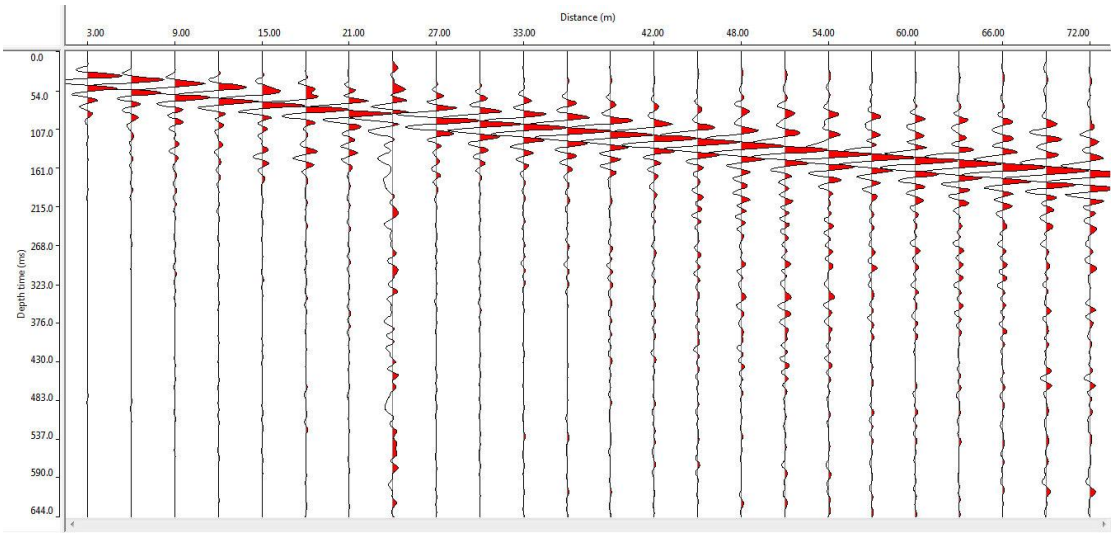

Figure.18. mean of five shot traces.

3-4. Data Processing and Inversion

Data processing consists of three steps (Figure 19):

1) Preliminary detection of surface waves,

2) Constructing the dispersion image panel and extracting the signal dispersion curve (strong power),

3) Back-calculating Vs variation with depth.

All these steps can be fully automated using SWAN software. The preliminary detection of surface waves examines recorded seismic waves in the most probable range of frequencies and phase velocities. Construction of the image panel is accomplished through a 2-D (time and space) wavefield transformation method that employs several pattern-recognition approaches (Park et al., 1998b). This transformation eliminates all the ambient cultural noise as well as source-generated noise such as scattered waves from buried objects (building foundations, culverts, boulders, etc.). The image panel shows the relation-ship between phase velocity and frequency for those waves propagated horizontally and directly from the impact point to the receiver line. The necessary dispersion curve, such as that of fundamental-mode Rayleigh waves, is then extracted from the energy accumulation pattern in this image panel (Figure 19) high energy. The extracted dispersion curve is finally used as a reference to back-calculate the Vp and Vs variation with depth below the surveyed area. This back calculation is called inversion and the process can be automated with reasonable constraints (Xia et al., 1999).

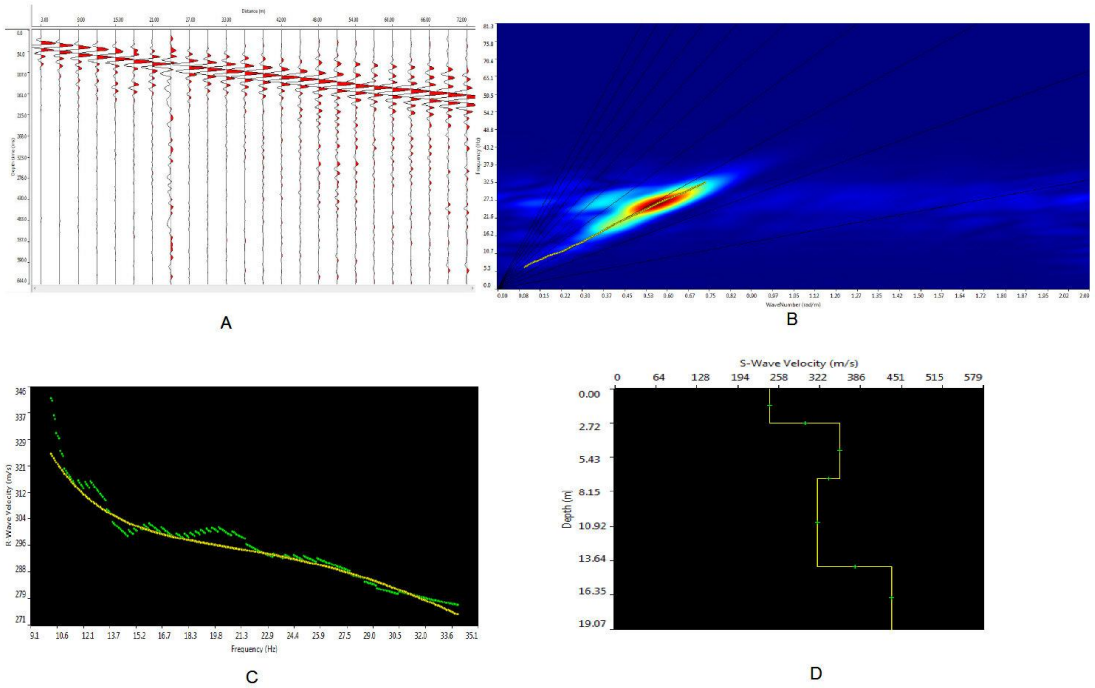

Figure.19. Illustrate data processing steps:
A: Mean field data mesurments
B: Constructing & extracted the dispersion curve
C: Matched measured and calculated dipersion curves
D: Shear wave velocity profile

3-5. Results:

The final 1D MASW model presented in table 19, four layers were distinguished.

Table.19.

Layer NO	Thick	Depth (m)	Vp	Vs	Density	Poisson	G (MPa)	E (MPa)
1	2.7	0-2.7	488	244	1.8	0.33	107.1648	285.0584
2	1.7	2.7-4.4	707	354	1.8	0.33	225.5688	600.013
3	2.6	4.4-7	638	319	1.8	0.33	183.1698	487.2317
4	7	7-14	871	436	1.8	0.33	342.1728	910.1796

The final 2D MASW model presented as cross section show changing in shear wave velocity (Vs) and compression wave velocity verses depth a long one cross section, figure 20 and figure 21.

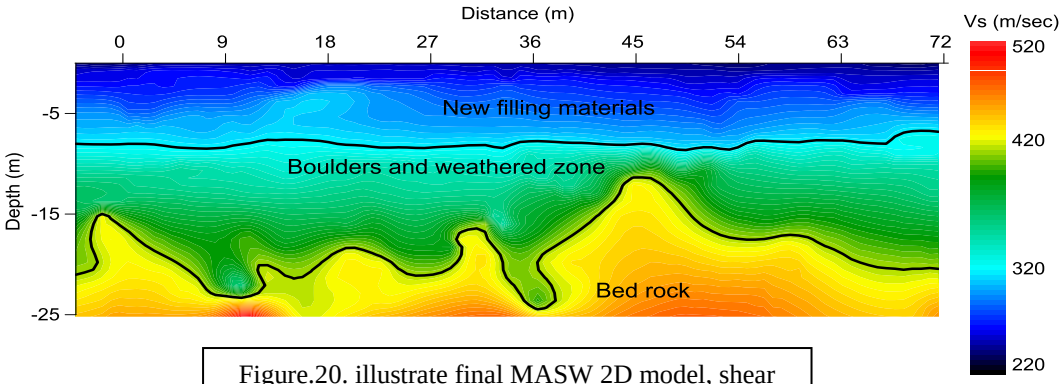

Figure.20. illustrate final MASW 2D model, shear wave velocity (stiffness cross section).

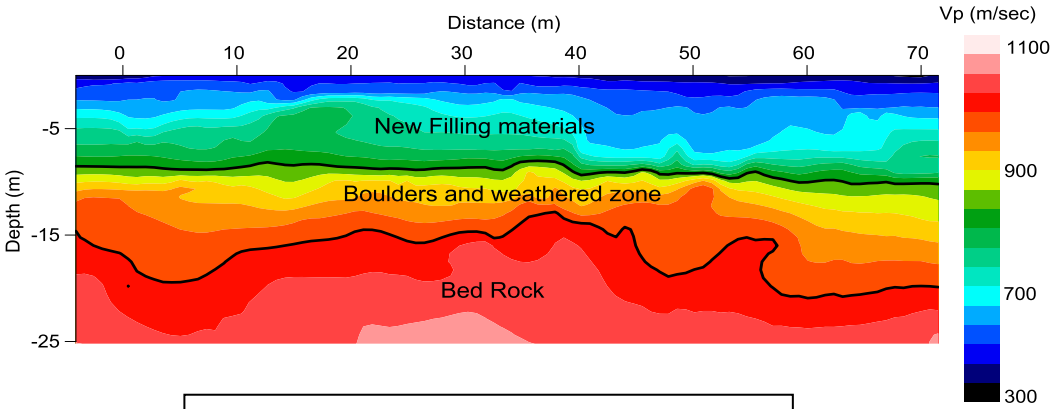

Figure.21. illustrate final MASW 2D model, comprision wave velocity.